Aircraft Flight Control Model using Computational Fluid Dynamics

Nattapat Srisom* Pakin Champasak* Sujin Bureerat** Natee Panagant[1]***

(Received: *May 7, 2020*; Revised: *August 15, 2020*; Accepted: *August 17, 2020*)

ABSTRACT

In aircraft design, one of the most critical aspects is aircraft stability and control, which needs to be considered with the utmost accuracy. Implementation of the software can increase the capability of the aircraft design, and also provide the effectiveness of working-time and saving other resources of the wind tunnel experiments. In this paper, computer code is developed for computing the stability and control derivatives for aircraft preliminary design by using aerodynamic coefficients, mass properties, and aircraft geometry. Moreover, the computer code can be used to generate an aircraft state-space model for the flight control design. The aerodynamic coefficients are estimated using computational fluid dynamic (CFD) software, while mass properties and aircraft geometry were carried out using computer-aid design (CAD) software. The proposed code was written using MATLAB computing language for efficient complex mathematical calculations while CFD analysis is performed via SOLIDWORKS software. The stability and control derivatives results of a transport aircraft model are evaluated with the code and compared to the results from Athena Vortex Lattice (AVL). At Mach 0.3, the results from the developed software are close to AVL with 16.36% of mean derivatives error. Due to transonic flow that cannot be captured by Vortex Lattice Method (VLM) in AVL, the error is increased to 20.64% and 22.50% at Mach 0.6 and Mach 0.8 respectively. The proposed software can be a high fidelity and efficient tool for aircraft design.

Keywords: Computational fluid dynamic, Stability and Control derivatives, State-space model

[1]*Corresponding author: natepa@kku.ac.th*

**Student, Master Engineering Program in Mechanical Engineering, Faculty of Engineering, Khon Kaen University, Thailand*

***Professor, Department of Mechanical Engineering, Faculty of Engineering, Khon Kaen University, Thailand*

****Lecturer, Department of Mechanical Engineering, Faculty of Engineering, Khon Kaen University, Thailand*

Introduction

In previous industrial development model, there is a lot of foreign company invested to manufacture technological products in Thailand. Anyways, an in-depth understanding of technologies is almost always keeping as secret and not transferred to Thai people, which caused Thailand to be stuck in the "Middle Income Trap". To stabilize the country, it is necessary to lift the new driving mechanisms by focusing on knowledge, science, technology, innovation, and creativity, which is known as Thailand 4.0 [1]. One of the national strategies was the development of unmanned aerial vehicles (UAVs) technology. UAVs can be used in a variety of missions such as resource exploration, monitoring of deforestation, national defence, etc. Therefore, the development of UAVs for both hardware and software aspects is an important part to fulfil the policy.

In aircraft design, computational fluid dynamic (CFD) plays a significant role in simulating airflow over a rigid and flexible component of an aircraft. To develop an accurate model of UAV flight dynamics, it is important to properly estimate its aerodynamic coefficients [2]. In design process, the software could compute the aerodynamic coefficients and reduce working time to use a wind tunnel test. For the completion of an aerodynamic study with an accurate estimation of aerodynamic coefficients, the theoretical analytical methods were performed along with CFD analysis [3]. The aerodynamic database must be provided for the configuration being studied, which then has to be combined with stability and control tools for analysis [4]. The accuracy of CFD can be validated with experimental measurements in the wind tunnel and flight testing [5]. A method that is traditionally used for aerodynamic calculation is the Vortex Lattice Method (VLM). VLM is implemented to compute stability and control derivatives of the isolated wing [6]. The control derivatives are the derivatives of aerodynamic parameters concerning the deflections of the ailerons, elevators, and a rudder that necessary for the aircraft stability and control design [7]. Stability and control derivatives can be obtained from many software programs for estimating data such as OpenVSP, CEASIOM, DATCOM, AVL etc. Such software is both freeware and commercialized. Open Vehicle Sketch Pad (OpenVSP) was used to generate parasite drag, trimmed stability for consideration of aircraft control [8]. Meanwhile, Conceptual Aircraft Design Tool (CEASIOM) has been developed to create stability and control data for basic aircraft design using different methods of accuracy for resulting in the dynamics of aerodynamics [9]. Athena Vortex Lattice (AVL) was used to generate dimensionless derivatives for medium altitude long endurance flights [10–13].

As most large commercial aircraft are operated in a transonic flight during the cruise phase, consequently, accurate aerodynamic performance is essential for the design process. Currently, VLM is widely used to evaluate aerodynamic performance in the aircraft's early design stages. VLM is classified as medium fidelity computation as its accuracy is reduced at transonic speed in cruise conditions. On the other hand, CFD is a higher fidelity method where flow analysis around an aircraft can be performed with higher accuracy. Although CFD required more computational resources, with recent computer technology, CFD analysis can be done within a reasonable time with a personal computer. CFD is widely used as a high fidelity tool for engineering design [14–17]. In this paper, a program code for higher fidelity aircraft design is developed. The code is capable of stability and control derivatives calculation and state-space generation. The software is developed in MATLAB programming language. An aircraft model is imported

from OpenVSP, then, it will be adjusted and refined in MATLAB while the SOLIDWORKS software is employed to be the CFD solver. Stability and control derivatives are calculated with the proposed code then compared to results obtained from AVL.

This paper includes introduction, objectives of the study, model and simulation, results and discussion, and conclusion sections. The model and simulation section separate into 4 subtopics include 1. Computer-aid design (CAD) 2. Computational fluid dynamics (CFD) 3. Aerodynamic stability and control derivatives and 4. State-space model.

Objectives of the study

1. To develop the program code that integrates OpenVSP and SOLIDWORKS for generating aircraft CAD models.
2. To develop the program code that generates stability and control derivatives as well as aircraft state-space models for both longitudinal and directional/lateral motions.
3. The program code was developed in an open-source format, which can be accessed by users for free.

Model and Simulation

In this paper, the aircraft model from OpenVSP (DegenGeom-file) is imported to MATLAB. The file consists of the outer surfaces of an aircraft, the internal structures e.g. wing ribs and spars, fuselage and other components were defined. Then, the aircraft model in the DegenGeom format is converted to a SOLIDWORKS model via the developed program code. After that, the aircraft aerodynamic coefficients are estimated by SOLIDWORKS flow simulation (CFD). After receiving the aerodynamic coefficients data, a comparison between CFD SOLIDWORKS Student Edition and AVL is made. Other than that, the computer code generates aerodynamic stability and control derivatives in order to enter the state-space model process.

Computer-Aid Design (CAD)

Computer-aid design is a method of applying computers to a drawing program, which is based on compelling geometry images to assemble into models. In the course of this process, aircraft components such as a fuselage, wings, elevators, and a rudder were built in a three-dimensional model. Each model was assembled into an aircraft model for determination of mass properties and aircraft geometry. The computer-aid design sequence was commanded by the developed computer code. In this paper, Boeing 737-200 model is considered as a case study.

Computational Fluid Dynamics (CFD)

In aircraft preliminary design, the computational fluid dynamic simulation responds to aerodynamic analyses leading to lift, drag, pitching moment, and the estimation of aerodynamic coefficients. This simulation exhibited the insight of flow field around or passing through of the aircraft, as well as a wide range of other analyses. In this paper, the SOLIDWORKS simulation software is used to simulate aerodynamic coefficients with the following conditions.

The process is shown in Figure 1.

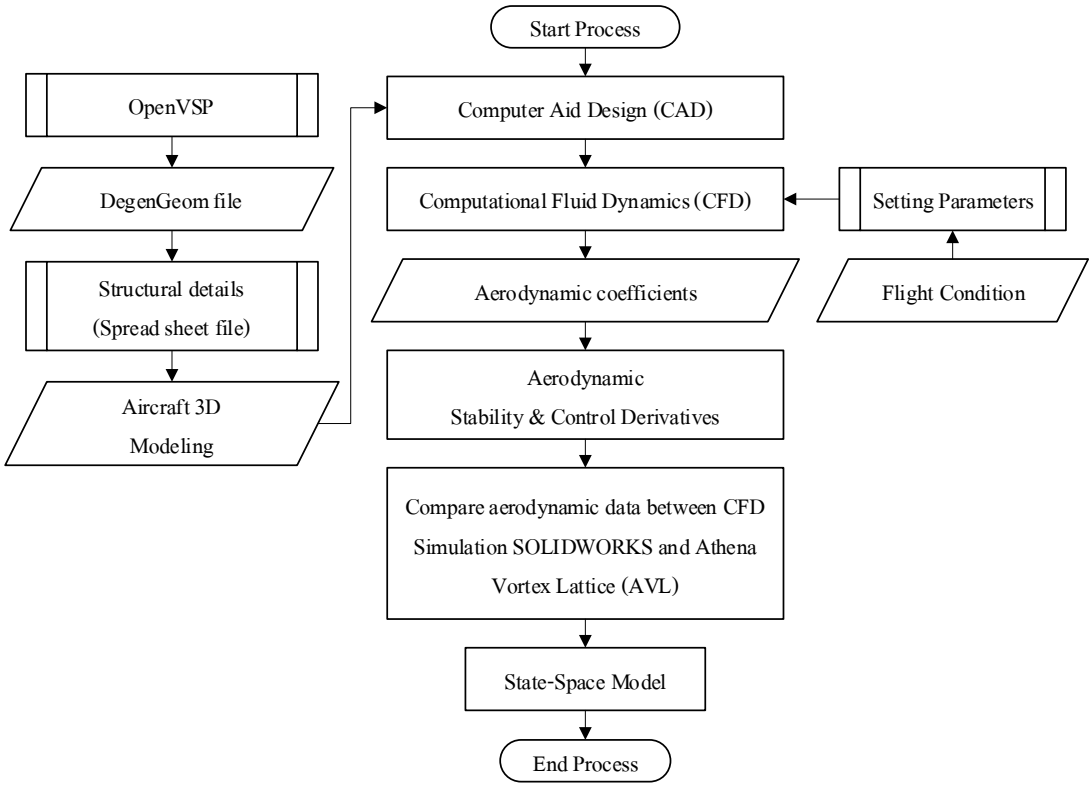

Figure 1 Aircraft flight control model process

The aircraft is shown in Figure 2 where the inertial and other related properties are given as:

$S = 106.378\ \text{m}^2$ $\bar{c} = 3.04\ \text{m}.$ $b = 34.95\ \text{m}.$ $X_{cg} = 16.149$

$X_{ac} = 12.969$ $\alpha = 4\ deg.$ $l_{xx} = 3.15x10^5\ \text{kg m}^2$ $l_{yy} = 45.1x10^5\ \text{kg m}^2$

$l_{zz} = 42.9x10^5\ \text{kg m}^2$ $l_{xz} = -12.6\ \text{kg m}^2$ $e = 0.8494$ $l_t = 15.58\ \text{m}.$ $S_t = 22.5\ \text{m}^2$

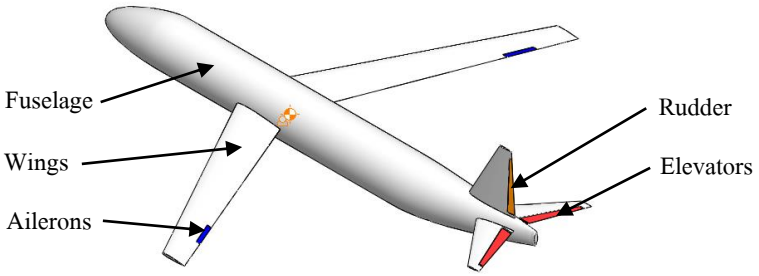

Figure 2 CAD modeling of Boeing 737-200

For the conditions of CFD simulation, computational domain and Mesh setting are shown in Table 1 and Figure 3. The aerodynamic forces and the direction of air flow are shown in Figure 4.

Table 1 The condition for simulate

Analysis type	External flow	Initial and ambient conditions	
	Exclude cavities without flow conditions	Altitude	8500 m.
	Exclude internal space	Pressure	33098.64 Pa
Fluids	Air (Gases)	Density	0.4951 kg/m^3
Flow type	Laminar and Turbulent	Velocity	Mach 0.3, 0.6 and 0.8
Wall conditions	Adiabatic wall	Turbulence intensity	1%
Roughness	0 micrometer	Angle of attack	-1 to 10 degrees
Humidity	Exclude	Control surface angle	-1 to 5 degrees

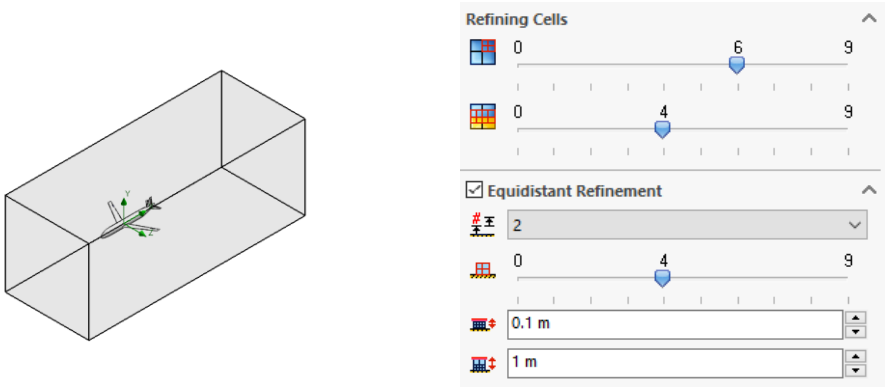

Figure 3 Computational domain (left) and Mesh setting (right)

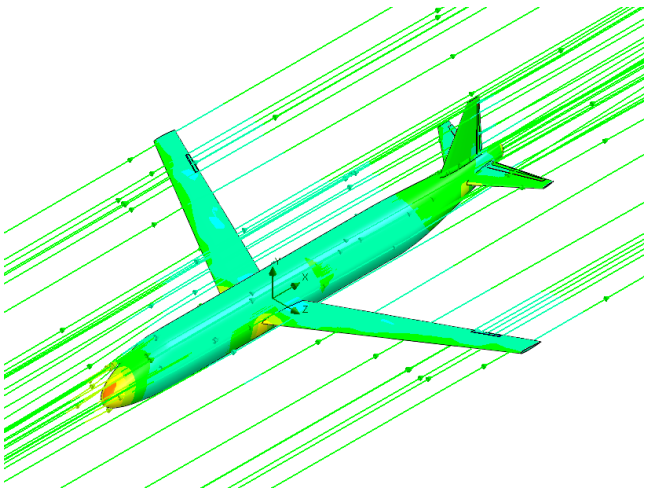

Figure 4 The aerodynamic force and direction of airflow

Estimation of force coefficient

- Lift coefficient

$$C_L = \frac{L}{QS}$$

- Drag coefficient

$$C_D = \frac{D}{QS}$$

Estimation of aerodynamic moment coefficient

- Rolling moment coefficient

$$C_l = \frac{l}{QSb}$$

- Yawing moment coefficient

$$C_n = \frac{N}{QSb}$$

- Pitching moment coefficient

$$C_m = \frac{M}{QS\bar{c}}$$

where *L, D, l, N, M* are the lift force, drag force, rolling, yawing and pitching moment, respectively.

Aerodynamic Stability and Control Derivatives

Aerodynamic stability and control derivatives are measured as the rate of changes of forces due to aircraft translational and rotational positions and control surface deflections. These parameters may change over time depending on the environment. Therefore, the stability and control derivatives are used for reducing the complexity of the swing equation and measuring the impact of changes in flight conditions while controlling derivatives effects in surface position control. In this process, the computer code used the aerodynamic coefficients from CFD simulation to compute the derivative values. The notation body axes that were changed are shown in Figure 5 while the equations are obtained from [18].

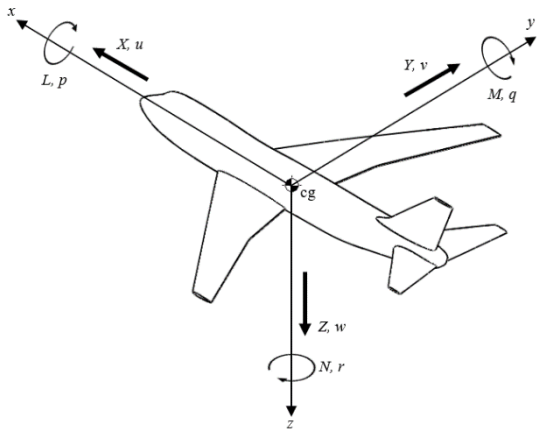

Figure 5 Notation for body axes. [X, Y, Z] = components of resultant aerodynamic force. [u, v, w] = components of velocity relative to atmosphere. L = rolling moment, M = pitching moment, N = yawing moment, p = rate of roll, q = rate of pitch, r = rate of yaw

Longitudinal stability derivatives

The longitudinal stability derivatives are calculated by using the longitudinal stability coefficients (Table 2) and the longitudinal dimensional stability derivatives (Table 3), respectively.

Table 2 The longitudinal stability coefficients

Variable	X-force derivatives	Z-force derivatives	Pitching moment derivatives
u	$C_{X_u} = C_{T_u} - MC_{D_M}$	$C_{Z_u} = -\frac{M^2}{1-M^2}C_{L_0}$	$C_{m_u} = M\frac{\partial C_m}{\partial M}$
α	$C_{X_\alpha} = C_{L_0} - C_{D_\alpha}$	$C_{Z_\alpha} = -(C_{L_\alpha} + C_{D_0})$	$C_{m_\alpha} = \frac{\partial C_m}{\partial \alpha}$
$\dot{\alpha}$	Neg.	$* C_{Z_{\dot{\alpha}}} = -2\eta_h V_H a_t \frac{d\varepsilon}{d\alpha}$	$* C_{m_{\dot{\alpha}}} = \frac{l_t}{\bar{c}} C_{Z_{\dot{\alpha}}}$
q	Neg.	$* C_{Z_q} = -C_{L_q}$	$* C_{m_q} = -\frac{l_t}{\bar{c}} C_{L_q}$

Neg. means usually negligible and (*) means the contribution of *tail only*.

M means Flight Mach number

where: $C_{T_u} = -2C_{D_0} - 2C_{L_0}\tan\Theta_0$ for constant thrust.

$C_{T_u} = -3C_{D_0} - 3C_{L_0}\tan\Theta_0$ for constant power.

$C_{L_\alpha} = (C_{L_i} - C_{L_0})/\alpha$ α at consider condition.

$C_{D_\alpha} = (C_{D_i} - C_{D_0})/\alpha$ α at consider condition.

$V_H = \ell_t S_t / S\bar{c}$ The horizontal tail volume ratio.

Table 3 The longitudinal dimensional stability derivatives

Variable	X	Z	M
u	$X_u = -\frac{QS}{mu_0}[2C_{D0} + MC_{D_M}]$	$Z_u = -\frac{QS}{mu_0}[2C_{L0} - C_{Zu}]$	$M_u = \frac{QS\bar{c}}{I_{yy}u_0} C_{mu}$
w	$X_w = \frac{QS}{mu_0} C_{X_\alpha}$	$Z_u = \frac{QS}{mu_0} C_{Z_\alpha}$	$M_w = \frac{QS\bar{c}}{I_{yy}u_0} C_{m_\alpha}$
$\dot{w}$	$X_{\dot{w}} = 0$	$Z_{\dot{w}} = \frac{QS\bar{c}}{2mu_0{}^2} C_{Z\dot{\alpha}}$	$M_{\dot{w}} = \frac{QS\bar{c}^2}{2I_{yy}u_0{}^2} C_{m\dot{\alpha}}$
q	$X_q = 0$	$Z_q = \frac{QS\bar{c}}{2mu_0} C_{Zq}$	$M_q = \frac{QS\bar{c}^2}{2I_{yy}u_0} C_{mq}$

u_0 mean velocity and m mean mass.

where: $C_{X_\alpha} = -2C_{D_\alpha} + C_{L_0}$ and $C_{Z_\alpha} = -C_{D_0} - C_{L_\alpha}$

Lateral / Directional stability derivatives

The lateral/directional stability derivatives were calculated by using the lateral/directional stability coefficients (Table 4) and the lateral/directional dimensional stability derivatives (Table 5), respectively.

Table 4 The lateral/directional stability coefficients

Variable	Y-force derivatives	Yawing moment derivatives	Rolling moment derivatives
β	$C_{y_\beta} = \frac{\partial C_y}{\partial \beta}$	$C_{l_\beta} = \frac{\partial C_l}{\partial \beta}$	$C_{n_\beta} = \frac{\partial C_n}{\partial \beta}$
p	$C_{y_p} = \left(\frac{2V_v}{b}\right)\frac{\partial C_y}{\partial P}$	$C_{l_p} = \left(\frac{2V_v}{b}\right)\frac{\partial C_l}{\partial P}$	$C_{n_p} = \left(\frac{2V_v}{b}\right)\frac{\partial C_n}{\partial P}$
r	$C_{y_r} = \left(\frac{2V_v}{b}\right)\frac{\partial C_y}{\partial R}$	$C_{l_r} = \left(\frac{2V_v}{b}\right)\frac{\partial C_l}{\partial R}$	$C_{n_r} = \left(\frac{2V_v}{b}\right)\frac{\partial C_n}{\partial R}$

where: $V_v = \ell_v S_v / Sb$ The vertical tail volume ratio.

Table 5 The lateral/directional dimensional stability derivatives

Variable	Y	L	N
v	$Y_v = \frac{QS}{mu_0} C_{y\beta}$	$L_v = \frac{QSb}{I_{xx}u_0} C_{l\beta}$	$N_v = \frac{QSb}{I_{zz}u_0} C_{n\beta}$
p	$Y_p = \frac{QSb}{2mu_0} C_{yp}$	$L_p = \frac{QSb^2}{2I_{xx}u_0} C_{lp}$	$N_p = \frac{QSb^2}{2I_{zz}u_0} C_{np}$
r	$Y_r = \frac{QSb}{2mu_0} C_{yr}$	$L_r = \frac{QSb^2}{2I_{xx}u_0} C_{lr}$	$N_r = \frac{QSb^2}{2I_{zz}u_0} C_{nr}$

Control derivatives

The control derivatives were the rates of change in forces and moments due to the deflections of elevators, ailerons and a rudder. The calculation of control derivatives is carried out similar to that of stability derivatives. The dimensional derivatives (Table 7 and Table 9) were calculated by using the values of the coefficients (Table 6 and Table 8).

Table 6 The longitudinal control coefficients

Variable	X-force derivatives	Z-force derivatives	Pitching moment derivatives
δ_e	Neg.	$C_{L_{\delta_e}} = \frac{\partial C_L}{\partial \delta_e}$	$C_{m_{\delta_e}} = \frac{\partial C_m}{\partial \delta_e}$

Table 7 The longitudinal dimensional control derivatives

Variable	X	Z	M
δ_e	$X_{\delta_e} = 0$	$Z_{\delta_e} = -\frac{S_t}{S} C_{L_{\delta_e}}$	$M_{\delta_e} = \frac{QS\bar{c}}{I_{yy}} C_{m_{\delta_e}}$

Table 8 The lateral/directional control coefficients

Variable	Y-force derivatives	Yawing moment derivatives	Rolling moment derivatives
δ_a	Neg.	$C_{n_{\delta_a}} = \frac{\partial C_{n_w}}{\partial \delta_a}$	$C_{l_{\delta_a}} = \frac{\partial C_{l_w}}{\partial \delta_a}$
δ_r	$C_{y_{\delta_r}} = \frac{\partial C_{y_v}}{\partial \delta_r}$	$C_{n_{\delta_r}} = \frac{\partial C_{n_v}}{\partial \delta_r}$	$C_{l_{\delta_r}} = \frac{\partial C_{l_v}}{\partial \delta_r}$

Table 9 The lateral/directional dimensional control derivatives

Variable	Y	N	L
δ_a	$Y_{\delta_a} = 0$	$N_{\delta_a} = \frac{QSb}{I_{zz}} C_{n_{\delta_a}}$	$L_{\delta_a} = \frac{QSb}{I_{xx}} C_{l_{\delta_a}}$
δ_r	$Y_{\delta_r} = \frac{S_F}{S} C_{y_{\delta_r}}$	$N_{\delta_r} = \frac{QSb}{I_{zz}} C_{n_{\delta_r}}$	$L_{\delta_r} = \frac{QSb}{I_{xx}} C_{l_{\delta_r}}$

State-Space Model

Aircraft motion is governed by Newton's second law observed from the northeast down inertia frame with help from using the body coordinates. The resulting equations of motions are nonlinear which are difficult to implement in reality. As a result, a small disturbance approach is employed to linearize the equations leading to a linear time-invariant state-space model. With the left-right symmetry of the aircraft, the model can be further simplified to have two state space systems for longitudinal and directional/lateral motions. The state-space model is a mathematical characteristic of plane changes in terms of ordinary linear differential equations with constant coefficients. The coefficients of the equations are the derivatives of aerodynamic force and moment. The two state-space models are expressed as follows:

Longitudinal motions

The longitudinal state variable vector: $\mathbf{x} = [u\ w\ q\ \theta]^T$

The longitudinal control vector: $\boldsymbol{\eta} = [\delta_e\ \delta_T]^T$

The system of first-order equations in standard form: $\dot{\boldsymbol{x}} = \mathbf{A}\boldsymbol{x} + \mathbf{B}\boldsymbol{\eta}$

where $\dot{x}$ represents the time derivative of the state vector x. In this case, the matrix A and B can be estimated from the longitudinal dimensional stability derivatives (Table 3) and the longitudinal dimensional control derivatives (Table 7).

$$\mathbf{A} = \begin{pmatrix} X_u & X_w & 0 & -g_0 \cos\Theta_0 \\ Z_u & Z_w & u_0 & -g_0 \sin\Theta_0 \\ M_u + M_{\dot{w}} Z_u & M_w + M_{\dot{w}} Z_w & M_q + u_0 Z_u & -M_{\dot{w}} g_0 \sin\Theta_0 \\ 0 & 0 & 1 & 0 \end{pmatrix}$$

$$\mathbf{B} = \begin{pmatrix} X_{\delta_e} & X_{\delta_T} \\ Z_{\delta_e} & Z_{\delta_T} \\ M_{\delta_e} + M_{\dot{w}} Z_{\delta_e} & M_{\delta_T} + M_{\dot{w}} Z_{\delta_T} \\ 0 & 0 \end{pmatrix}$$

Lateral / Directional motions

The system of first-order equations is similar to longitudinal motions. But the matrices are changed by directions. Matrix A and B can be estimated from the lateral/ directional dimensional stability derivatives (Table 4) and the lateral/directional dimensional control derivatives (Table 9).

The lateral/directional state variable vector: $\mathbf{x} = [v\ p\ r]^T$

The lateral/directional control vector: $\boldsymbol{\eta} = [\delta_r\ \delta_a]^T$

$$\mathbf{A} = \begin{pmatrix} Y_v & Y_p & g_0 \cos\Theta_0 & Y_r - u_0 \\ L_v & L_p & 0 & L_r \\ 0 & 1 & 0 & 0 \\ N_v & N_p & 0 & N_r \end{pmatrix}$$

$$\mathbf{B} = \begin{pmatrix} Y_{\delta_r} & 0 \\ L_{\delta_r} & L_{\delta_a} \\ 0 & 0 \\ N_{\delta_r} & N_{\delta_a} \end{pmatrix}$$

Results and Discussion

In this paper, the Boeing 737-200 model is considered as a case study and for comparison of the aerodynamic data between that obtained from using CFD (SOLIDWORKS) and VLM by using AVL. The results are estimated by the same inertial and other related properties, whereas simulation at Mach 0.3, 0.6, and 0.8 are performed.

From the results at Mach 0.3 in Table 10, results from the proposed software are close to AVL with 16.36% mean error. Almost all coefficients have percentage error less than 30%. But since AVL used VLM to compute lift and drag forces, it can only capture induced drag while parasite drag caused by friction is neglected. Therefore, this causes the percentage error of some coefficients such as C_D, C_{D_α} and C_{n_β} still obviously higher compared to other coefficients at low speed.

For higher speed at Mach 0.6 (Table 11) and transonic speed at Mach 0.8 (Table 12), the mean errors are increased to 20.64% and 22.50% respectively. There are 4 and 7 out of 14 coefficients that have more than 30% error in Mach 0.6 and Mach 0.8 respectively. It should be noted that from assumptions used in VLM, some phenomena in transonic regimes such as flow separation or shockwave cannot be captured. Thus, derivatives calculation with flow results from CFD uses Reynolds Averaged Navier Stokes (RANS) equation with turbulence modeling [19] in the proposed method should have more accuracy than VLM.

Table 10 The comparison of aerodynamic coefficients at speed Mach 0.3

Aerodynamic Coefficients	Athena Vortex Lattice (AVL)	SOLIDWORKS Flow Simulation	Difference Values	% Error
C_L	0.3869	0.3595	0.0274	7
C_D	0.0216	0.0689	0.0473	31
C_{L_α}	5.6143	4.4798	1.1345	20
C_{D_α}	0.0951	0.0590	0.0361	38

Table 10 The comparison of aerodynamic coefficients at speed Mach 0.3 (Cont.)

Aerodynamic Coefficients	Athena Vortex Lattice (AVL)	SOLIDWORKS Flow Simulation	Difference Values	% Error
C_{m_α}	-4.8498	-3.8572	0.9926	20
C_{L_q}	21.377	20.5349	0.8421	4
C_{m_q}	-83.711	-76.7022	7.0080	8
C_{y_β}	-0.6766	-0.5246	0.1520	22
C_{l_β}	-0.1368	-0.1576	0.0208	15
C_{n_β}	0.0598	0.0223	0.0375	37
C_{l_p}	-0.5325	-0.5840	0.0515	10
C_{n_p}	-0.0445	-0.0024	0.0421	5
C_{l_r}	0.1374	0.1362	0.0013	1
C_{n_r}	-0.2346	-0.1956	0.0390	11
			Mean % Error	16.36

Table 11 The comparison of aerodynamic coefficients at speed Mach 0.6

Aerodynamic Coefficients	Athena Vortex Lattice (AVL)	SOLIDWORKS Flow Simulation	Difference Values	% Error
C_L	0.4292	0.3114	0.1178	27
C_D	0.0234	0.0314	0.0080	34
C_{L_α}	6.1914	3.5197	2.6717	43
C_{D_α}	0.1277	0.0332	0.0945	26
C_{m_α}	-5.4029	-4.3957	1.0072	19
C_{L_q}	23.1240	23.2109	0.0869	0
C_{m_q}	-90.5635	-86.1489	4.4146	5
C_{y_β}	-0.6952	-0.4130	0.2822	41
C_{l_β}	-0.1511	-0.1381	0.0130	9
C_{n_β}	0.0680	0.0216	0.0464	32
C_{l_p}	-0.5789	-0.6659	0.0870	15
C_{n_p}	-0.0498	-0.0018	0.0480	2
C_{l_r}	0.1515	0.1876	0.0361	24
C_{n_r}	-0.2459	-0.2161	0.0298	12
			Mean % Error	20.64

Table 12 The comparison of aerodynamic coefficients at speed Mach 0.8

Aerodynamic Coefficients	Athena Vortex Lattice (AVL)	SOLIDWORKS Flow Simulation	Difference Values	% Error
C_L	0.4969	0.3441	0.1528	31
C_D	0.0256	0.0689	0.0433	37
C_{L_α}	7.1061	4.8241	2.2820	32
C_{D_α}	0.2020	0.6136	0.4116	33
C_{m_α}	-6.2739	-5.3604	0.9135	15
C_{L_q}	25.7795	28.0032	2.2237	9
C_{m_q}	-101.1276	-103.0515	1.9239	2
C_{y_β}	-0.7199	-0.4621	0.2578	36
C_{l_β}	-0.1731	-0.2243	0.0512	30
C_{n_β}	0.0797	0.0469	0.0241	30
C_{l_p}	-0.6477	-0.8188	0.1711	26
C_{n_p}	-0.0579	-0.0011	0.0568	2
C_{l_r}	0.1734	0.1468	0.0266	25
C_{n_r}	-0.2616	-0.2443	0.0173	7
			Mean % Error	22.50

In the calculation of SOLIDWORKS Flow Simulation, the aerodynamic coefficient was affected by the total of element cells and fluid contract cells. Mesh analysis is performed to ensure accurate results with a minimize number of elements/ cells as possible. Results of 3 conditions mesh quality are displayed in Table 12. The aerodynamic coefficient results are converged after number fluid contract cells larger than 0.7 million. The C_L, C_D, and C_m results of condition 2 have only about 3.4%, 5.6%, and 5.8% error respectively compared to condition 3.

Table 13 Constraint condition for estimating aerodynamic values

	Condition 1	Condition 2	Condition 3
Total element cell	0.7 million	2.6 million	5.3 million
Fluid contract cell	0.2 million	0.7 million	0.85 million
C_L	0.2854	0.3595	0.3722
C_D	0.0300	0.0245	0.0232
C_m	-0.1004	-0.0469	-0.0498

State-Space model

After aerodynamic coefficients are calculated from the comparison of aerodynamic coefficients at speed Mach 0.8 (Table 12), a state-space model is formed as follows:

- The longitudinal plant matrix:

$$\mathbf{A} = \begin{pmatrix} -0.2540 & -0.3592 & 0 & -9.7820 \\ -1.6173 & -6.2118 & 205.2662 & 0 \\ 0.0002 & -0.0295 & -0.7793 & 0 \\ 0 & 0 & 1.0000 & 0 \end{pmatrix}$$

$$\mathbf{B} = \begin{pmatrix} 0 \\ -0.1142 \\ -2.6162 \\ 0 \end{pmatrix}$$

- The lateral / directional plant matrix:

$$\mathbf{A} = \begin{pmatrix} -0.6159 & 3.9077 & 9.7820 & -259.5287 \\ -0.1784 & -8.9924 & 0 & 2.5601 \\ 0 & 1.0000 & 0 & 0 \\ 0.0029 & -0.0011 & 0 & -0.2666 \end{pmatrix}$$

$$\mathbf{B} = \begin{pmatrix} 0.0168 & 0 \\ 1.0469 & 7.2328 \\ 0 & 0 \\ -0.9608 & -0.0472 \end{pmatrix}$$

Conclusions

The program code written in MATLAB for computer-aided aircraft design is developed. The program integrates OpenVSP and SOLIDWORKs for generating aircraft CAD models, stability and control derivatives as well as aircraft state-space models for both longitudinal and directional/lateral motions. It can be easily extended for other CFD software. The result in estimating stability and control derivatives by the proposed software is reasonably close to results from AVL at low speed and the difference between both methods are greater at transonic speed. The comparative results between the proposed code and the AVL code reveal that the code can, to some extent, provide reasonable results. It should be noted that the degree of accuracy depends on the CFD software used, which in this study is SOLIDWORKs simulation. For future work, results of the proposed software will be validated to high fidelity software or experimental data to further ensure its accuracy.

Acknowledgments

This study was supported by all personnel in Department of Mechanical Engineering Khon Kaen University.

References

1. Contributions A. AMCHAM CONTRIBUTIONS TO THAILAND 4 . 0 AMCHAM WHITE PAPER – CONTRIBUTIONS TO THAILAND 4 . 0. :1–9.
2. Kuitche M, Segui M, Botez RM, Gabor OS, Ghazi G. New methodology for flight dynamics modeling of the UAS-S4 Ehécatl towards its aerodynamics estimation modeling. AIAA Model Simul Technol Conf 2017. 2017;(March).
3. Panagiotou P, Tsavlidis I, Yakinthos K. Conceptual design of a hybrid solar MALE UAV. Aerosp Sci Technol [Internet]. 2016;53:207–19. Available from: http://dx.doi.org/10.1016/j.ast.2016.03.023
4. Rizzi A. Modeling and simulating aircraft stability and control - The SimSAC project. Prog Aerosp Sci [Internet]. 2011;47(8):573–88. Available from: http://dx.doi.org/10.1016/j.paerosci.2011.08.004
5. Vallespin D, Badcock KJ, Da Ronch A, White MD, Perfect P, Ghoreyshi M. Computational fluid dynamics framework for aerodynamic model assessment. Prog Aerosp Sci [Internet]. 2012;52:2–18. Available from: http://dx.doi.org/10.1016/j.paerosci.2011.12.004
6. Piedra S, Martinez E, Escalante-Velazquez CA, Jimenez SMA. Computational aerodynamics analysis of a light-sport aircraft: Compliance study for stall speed and longitudinal stability certification requirements. Aerosp Sci Technol. 2018;
7. Houghton EL, Carruthers NB. Aerodynamics for engineering students. Third edition. 1982.
8. Freeman JL, Klunk GT. Dynamic Flight Simulation of Spanwise Distributed Electric Propulsion for Directional Control Authority. 2018 AIAA/IEEE Electr Aircr Technol Symp EATS 2018. 2018;4997.
9. Tomac M, Eller D. From geometry to CFD grids - An automated approach for conceptual design. Prog Aerosp Sci [Internet]. 2011;47(8):589–96. Available from: http://dx.doi.org/10.1016/j.paerosci.2011.08.005
10. Kadiri M, Mohammed A, Sanusi S. Validation of Aerodynamic Coefficients for Flight Control System of A Medium Altitude Long Endurance Unmanned Aerial vehicle. In: 2019 2nd International Conference of the IEEE Nigeria Computer Chapter, NigeriaComputConf 2019. 2019.
11. McKinnis A, Keshmiri S. Dynamic Modeling and Controllability Analysis of a Moderately Damaged Unmanned Aerial System. In: IEEE Aerospace Conference Proceedings. 2019.
12. Klausmeyer SM, Fisher C, Laflin K. Stability derivative estimation: Methods and practical considerations for conventional transonic aircraft. In: 2018 Applied Aerodynamics Conference. 2018.
13. McKinnis A, Schmitz I, Rose J, Phommachanh J, Hartwell B, Sargent M. Viking-400 uas dynamic analysis. AIAA Scitech 2019 Forum. 2019;2514.
14. Gu X, Ciampa PD, Nagel B. An automated CFD analysis workflow in overall aircraft design applications. CEAS Aeronaut J. 2018;9(1):3–13.
15. Leifsson L, Koziel S, Bekasiewicz A. Fast low-fidelity wing aerodynamics model for surrogate-based shape optimization. Procedia Comput Sci [Internet]. 2014;29:811–20. Available from: http://dx.doi.org/10.1016/j.procs.2014.05.073

16. Mialon B, Khrabrov A, Khelil S Ben, Huebner A, Da Ronch A, Badcock K, et al. Validation of numerical prediction of dynamic derivatives: The DLR-F12 and the Transcruiser test cases. Prog Aerosp Sci. 2011;47(8):674–694.
17. GUO X, FAN B, HUANG J, XIE J. CFD and VLM Simulation of the Novel Twin-body Asymmetric Flying-wing Aircraft. DEStech Trans Comput Sci Eng. 2020;(msam).
18. Caughey DA. Introduction to Aircraft Stability and Control Course Notes. 2011;153.
19. Profile SEE. COMPARING VLM AND CFD MANEUVER LOADS CALCULATIONS. 2019;(June).

Nomenclature

α	Angle of attack	β	Angle of sideslip
θ	Pitch angle	φ	Roll angle
ψ	Yaw angle	Γ	Dihedral angle
p	Roll rate	q	Pitch rate
r	Yaw rate	u	Axial velocity
v	Lateral velocity	w	Normal velocity
δ_a	Aileron deflection	δ_e	Elevator deflection
δ_r	Rudder deflection	η	Efficiency factor of wing
η_h	Efficiency factor of tail	η_v	Efficiency factor of vertical tail
e	Oswald efficiency factor	a_t	The tail lift-curve slope.
a_v	The vertical tail lift-curve slope	cg.	Center of gravity
AR	Aspect ratio	M	Flight Mach number
S	Wing area	S_t	Horizontal tail area
S_v	Vertical tail area	$\overline{c}$	Mean aerodynamic chord
b	Wing span	b_v	Vertical tail span
X_{ac}	X position in aerodynamic chord	X_{ac}	X position in cg.
I_{xx}, I_{yy}, I_{zz}	Moment of inertias	I_{xy}, I_{xz}, I_{yz}	Product of inertia
l_t	Distance from center of gravity to tail quarter chord		
l_v	Distance from center of gravity to vertical tail quarter chord		
$\mathrm{d}\varepsilon/\mathrm{d}\alpha$	The rate of change of downwash with an angle of attack		
$\mathrm{d}\sigma/\mathrm{d}\beta$	The rate of change of side wash with an angle of sideslip		
z'_v	The distance of the vertical tail to dihedral effect		
C_{D_α}	Drag due to the angle of attack derivative		
C_{D_q}	Drag due to the pitch rate derivative		
$C_{D_{\dot{\alpha}}}$	Drag due to the angle of attack rate derivative		
C_{L_t}	Tail-lift coefficient		
C_{L_α}	Lift due to the angle of attack derivative		

C_{L_q}	Lift due to the pitch rate derivative
$C_{L_{\dot{\alpha}}}$	Lift due to the angle of attack rate derivative
$C_{L_{\delta_e}}$	Lift due to the angle of the elevator
C_{m_α}	Pitching moment due to the angle of attack derivative
C_{m_q}	Pitching moment due to the pitch rate derivative
$C_{m_{\dot{\alpha}}}$	Pitching moment due to the angle of attack rate derivative
$C_{m_{\delta_e}}$	Pitching moment due to the angle of the elevator
C_{l_p}	Rolling moment due to the roll rate derivative
C_{l_r}	Rolling moment due to the yaw rate derivative
C_{l_β}	Rolling moment due to the sideslip angle derivative
$C_{l_{\dot{\beta}}}$	Rolling moment due to the sideslip angle rate derivative
C_{l_v}	Rolling moment due to the lateral velocity
C_{l_w}	Rolling moment due to the normal velocity
C_{n_p}	Yawing moment due to the roll rate derivative
C_{n_r}	Yawing moment due to the yaw rate derivative
C_{n_β}	Yawing moment due to the sideslip angle derivative
$C_{n_{\dot{\beta}}}$	Yawing moment due to the sideslip angle rate derivative
C_{n_v}	Yawing moment due to the lateral velocity
C_{n_w}	Yawing moment due to the normal velocity
C_{y_p}	Side force due to the roll rate derivative
C_{y_r}	Side force due to the yaw rate derivative
C_{y_β}	Side force due to the sideslip angle derivative
$C_{y_{\dot{\beta}}}$	Side force due to the sideslip angle rate derivative
C_{y_v}	Side force due to the lateral velocity
C_{y_w}	Side force due to the normal velocity